



Production of Prompt Charmonia in e^+e^- Annihilation at $\sqrt{s} \approx 10.6 \text{ GeV}^*$

The Belle Collaboration

K. Abe⁹, K. Abe³⁹, T. Abe⁴⁰, I. Adachi⁹, Byoung Sup Ahn¹⁶, H. Aihara⁴¹, M. Akatsu²¹,
Y. Asano⁴⁶, T. Aso⁴⁵, T. Aushev¹⁴, A. M. Bakich³⁷, Y. Ban³², E. Banas²⁶, S. Behari⁹,
P. K. Behera⁴⁷, A. Bondar², A. Bozek²⁶, T. E. Browder⁸, B. C. K. Casey⁸, P. Chang²⁵,
Y. Chao²⁵, B. G. Cheon³⁶, R. Chistov¹⁴, S.-K. Choi⁷, Y. Choi³⁶, L. Y. Dong¹², J. Dragic¹⁹,
A. Drutskoy¹⁴, S. Eidelman², Y. Enari²¹, F. Fang⁸, H. Fujii⁹, C. Fukunaga⁴³,
M. Fukushima¹¹, N. Gabyshev⁹, A. Garmash^{2;9}, T. Gershon⁹, A. Gordon¹⁹, R. Guo²³,
J. Haba⁹, H. Hamasaki⁹, F. Handa⁴⁰, K. Hara³⁰, T. Hara³⁰, H. Hayashii²², M. Hazumi³⁰,
E. M. Heenan¹⁹, I. Higuchi⁴⁰, T. Hokuue²¹, Y. Hoshi³⁹, S. R. Hou²⁵, W.-S. Hou²⁵,
H.-C. Huang²⁵, Y. Igarashi⁹, T. Iijima⁹, H. Ikeda⁹, K. Inami²¹, A. Ishikawa²¹, H. Ishino⁴²,
R. Itoh⁹, H. Iwasaki⁹, Y. Iwasaki⁹, P. Jalocha²⁶, H. K. Jang³⁵, J. H. Kang⁵⁰, J. S. Kang¹⁶,
P. Kapusta²⁶, N. Katayama⁹, H. Kawai⁴¹, N. Kawamura¹, T. Kawasaki²⁸, H. Kichimi⁹,
D. W. Kim³⁶, Heejong Kim⁵⁰, H. J. Kim⁵⁰, H. O. Kim³⁶, Hyunwoo Kim¹⁶, S. K. Kim³⁵,
T. H. Kim⁵⁰, K. Kinoshita⁵, S. Kobayashi³⁴, H. Konishi⁴⁴, P. Krokovny², R. Kulasiri⁵,
S. Kumar³¹, A. Kuzmin², Y.-J. Kwon⁵⁰, J. S. Lange⁶, G. Leder¹³, S. H. Lee³⁵,
D. Liventsev¹⁴, R.-S. Lu²⁵, J. MacNaughton¹³, D. Marlow³³, T. Matsubara⁴¹,
S. Matsumoto⁴, T. Matsumoto²¹, Y. Mikami⁴⁰, K. Miyabayashi²², H. Miyake³⁰,
H. Miyata²⁸, G. R. Moloney¹⁹, S. Mori⁴⁶, T. Mori⁴, T. Nagamine⁴⁰, Y. Nagasaka¹⁰,
Y. Nagashima³⁰, E. Nakano²⁹, M. Nakao⁹, J. W. Nam³⁶, Z. Natkaniec²⁶, K. Neichi³⁹,
S. Nishida¹⁷, O. Nitoh⁴⁴, S. Noguchi²², T. Nozaki⁹, S. Ogawa³⁸, T. Ohshima²¹, T. Okabe²¹,
S. Okuno¹⁵, W. Ostrowicz²⁶, H. Ozaki⁹, P. Pakhlov¹⁴, H. Palka²⁶, C. S. Park³⁵,
C. W. Park¹⁶, H. Park¹⁸, K. S. Park³⁶, M. Peters⁸, L. E. Piilonen⁴⁸, N. Root²,
K. Rybicki²⁶, J. Ryuko³⁰, H. Sagawa⁹, Y. Sakai⁹, H. Sakamoto¹⁷, M. Satpathy⁴⁷,
A. Satpathy^{9;5}, S. Schrenk⁵, S. Semenov¹⁴, K. Senyo²¹, M. E. Sevier¹⁹, H. Shibuya³⁸,
B. Shwartz², S. Stanić⁴⁶, A. Sugiyama²¹, K. Sumisawa⁹, T. Sumiyoshi⁹, J.-I. Suzuki⁹,
K. Suzuki³, S. Suzuki⁴⁹, S. K. Swain⁸, T. Takahashi²⁹, F. Takasaki⁹, M. Takita³⁰,
K. Tamai⁹, N. Tamura²⁸, J. Tanaka⁴¹, M. Tanaka⁹, Y. Tanaka²⁰, G. N. Taylor¹⁹,
Y. Teramoto²⁹, M. Tomoto⁹, T. Tomura⁴¹, S. N. Tovey¹⁹, K. Trabelsi⁸, W. Trischuk^{33;†},
T. Tsuboyama⁹, T. Tsukamoto⁹, S. Uehara⁹, K. Ueno²⁵, Y. Unno³, S. Uno⁹, Y. Ushiroda⁹,

*submitted to PRL

S. E. Vahsen³³, K. E. Varvell³⁷, C. C. Wang²⁵, C. H. Wang²⁴, J. G. Wang⁴⁸, M.-Z. Wang²⁵,
Y. Watanabe⁴², E. Won³⁵, B. D. Yabsley⁹, Y. Yamada⁹, M. Yamaga⁴⁰, A. Yamaguchi⁴⁰,
Y. Yamashita²⁷, M. Yamauchi⁹, K. Yoshida²¹, Y. Yuan¹², Y. Yusa⁴⁰, C. C. Zhang¹²,
J. Zhang⁴⁶, H. W. Zhao⁹, Y. Zheng⁸, V. Zhilich², and D. Žontar⁴⁶

¹Aomori University, Aomori

²Budker Institute of Nuclear Physics, Novosibirsk

³Chiba University, Chiba

⁴Chuo University, Tokyo

⁵University of Cincinnati, Cincinnati OH

⁶University of Frankfurt, Frankfurt

⁷Gyeongsang National University, Chinju

⁸University of Hawaii, Honolulu HI

⁹High Energy Accelerator Research Organization (KEK), Tsukuba

¹⁰Hiroshima Institute of Technology, Hiroshima

¹¹Institute for Cosmic Ray Research, University of Tokyo, Tokyo

¹²Institute of High Energy Physics, Chinese Academy of Sciences, Beijing

¹³Institute of High Energy Physics, Vienna

¹⁴Institute for Theoretical and Experimental Physics, Moscow

¹⁵Kanagawa University, Yokohama

¹⁶Korea University, Seoul

¹⁷Kyoto University, Kyoto

¹⁸Kyungpook National University, Taegu

¹⁹University of Melbourne, Victoria

²⁰Nagasaki Institute of Applied Science, Nagasaki

²¹Nagoya University, Nagoya

²²Nara Women's University, Nara

²³National Kaohsiung Normal University, Kaohsiung

²⁴National Lien-Ho Institute of Technology, Miao Li

²⁵National Taiwan University, Taipei

²⁶H. Niewodniczanski Institute of Nuclear Physics, Krakow

²⁷Nihon Dental College, Niigata

²⁸Niigata University, Niigata

²⁹Osaka City University, Osaka

³⁰Osaka University, Osaka

³¹Panjab University, Chandigarh

³²Peking University, Beijing

³³Princeton University, Princeton NJ

³⁴Saga University, Saga

³⁵Seoul National University, Seoul

³⁶Sungkyunkwan University, Suwon

³⁷University of Sydney, Sydney NSW

³⁸Toho University, Funabashi

³⁹Tohoku Gakuin University, Tagajo

⁴⁰Tohoku University, Sendai

⁴¹University of Tokyo, Tokyo

⁴²Tokyo Institute of Technology, Tokyo

⁴³Tokyo Metropolitan University, Tokyo

⁴⁴Tokyo University of Agriculture and Technology, Tokyo

⁴⁵Toyama National College of Maritime Technology, Toyama

⁴⁶University of Tsukuba, Tsukuba

⁴⁷Utkal University, Bhubaneswer

⁴⁸Virginia Polytechnic Institute and State University, Blacksburg VA

⁴⁹Yokkaichi University, Yokkaichi

⁵⁰Yonsei University, Seoul

[†]on leave from University of Toronto, Toronto ON

Abstract

The production of prompt J/ψ , $\psi(2S)$, χ_{c1} and χ_{c2} is studied using a 32.4 fb^{-1} data sample collected with the Belle detector at the $\Upsilon(4S)$ and 60 MeV below the resonance. The yield of prompt J/ψ mesons in the $\Upsilon(4S)$ sample is compatible with that of continuum production; we set an upper limit $\mathcal{B}(\Upsilon(4S) \rightarrow J/\psi X) < 1.9 \times 10^{-4}$ at the 95% confidence level, and find $\sigma(e^+e^- \rightarrow J/\psi X) = 1.47 \pm 0.10 \pm 0.13 \text{ pb}$. The cross-sections for prompt $\psi(2S)$ and direct J/ψ are measured. The J/ψ momentum spectrum, production angle distribution and polarization are studied.

PACS numbers: 13.65.+i, 13.25.Gv, 14.40.Gx

The production of prompt charmonia is poorly understood, and provides an interesting environment to study the interplay between perturbative QCD and non-perturbative effects. A recently developed effective field theory, called non-relativistic QCD (NRQCD) [1], provides a consistent calculational framework for direct heavy quarkonium production. Further experimental information is needed to establish the applicability of NRQCD to charmonium production [2]. Studies of prompt charmonia in e^+e^- collisions at the $\Upsilon(4S)$ resonance constitute a test of NRQCD and can provide estimates of some of its non-perturbative matrix elements.

In this Letter, we report results of a measurement of prompt charmonium production in data recorded at the $\Upsilon(4S)$ and in the continuum 60 MeV below the resonance, corresponding to integrated luminosities of 29.4 fb^{-1} and 3.0 fb^{-1} respectively [3]. The data was collected with the Belle detector at the KEKB asymmetric energy ($3.5 \text{ GeV} \times 8 \text{ GeV}$) e^+e^- storage ring [4].

The Belle detector is a large-solid-angle spectrometer equipped with a 1.5 T superconducting solenoid magnet. Charged tracks are reconstructed in a 50 layer Central Drift Chamber (CDC) and in three concentric layers of double sided silicon strip detectors (SVD). Photons and electrons are identified using a CsI(Tl) Electromagnetic Calorimeter (ECL) located inside the magnet coil. Muons and K_L^0 mesons are detected using resistive plate chambers embedded in the iron magnetic flux return (KLM). Charged particles are identified using specific ionization measurements in the CDC, pulse heights from the Aerogel Čerenkov Counters (ACC) and timing information from the Time of Flight Counters (TOF). A detailed description of the Belle detector can be found elsewhere [5].

Hadronic events are separated from QED, $\tau\tau$, two-photon and beam-gas interaction backgrounds by requiring the presence of at least three charged tracks ($N_{\text{ch}} \geq 3$), an event vertex with radial ($r\phi$) and z coordinates within 1.5 and 3.5 cm of the origin, respectively, a total reconstructed center-of-mass (CM) energy greater than $0.2\sqrt{s}$ (\sqrt{s} is the CM collision energy), a z component of the net reconstructed CM momentum less than $0.5\sqrt{s}/c$, a total ECL energy between $0.1\sqrt{s}$ and $0.8\sqrt{s}$ with at least two energy clusters associated, and R_2 , the ratio of second and zeroth Fox-Wolfram moments, less than 0.8.

Candidate J/ψ mesons are reconstructed using the leptonic decays $J/\psi \rightarrow \mu^+\mu^-$ and e^+e^- . For $J/\psi \rightarrow \mu^+\mu^-$, both charged tracks must be identified as muons in the KLM using information on hit positions and penetration depth. For $J/\psi \rightarrow e^+e^-$, oppositely charged track pairs must be identified as electrons based on a combination of CDC dE/dx information, ACC response, and the position, shape and energy of the associated ECL shower. To correct for final state radiation and bremsstrahlung, photons within 50 mrad of the e^\pm are included in the e^+e^- invariant mass calculation. The two lepton candidate tracks are required to have a common vertex, with a distance in the $r\phi$ plane to the average interaction point $d_{r\phi} < 500 \mu\text{m}$. The signal region is defined by the mass window $-93 < M_{l+l-} - M_{J/\psi} < 33 \text{ MeV}/c^2$, common for both decay channels.

We reconstruct $\psi(2S) \rightarrow J/\psi\pi^+\pi^-$ decays by combining J/ψ candidates with $\pi^+\pi^-$ pairs and requiring a common $\pi^+\pi^-$ vertex. Candidate χ_{c1} and χ_{c2} mesons are reconstructed via their radiative decays to the J/ψ : we combine J/ψ candidates with photons detected in the ECL, that are not associated with an identified π^0 .

The largest source of secondary charmonia in the $\Upsilon(4S)$ sample, due to B meson decays, is eliminated by requiring the charmonium CM momentum p^* to be above the B decay

kinematic limit. A common requirement $p^* > 2.0$ GeV/ c is used for all analyses (J/ψ , $\psi(2S)$, χ_{c1} and χ_{c2}): this value is robust against the effects of momentum measurement errors and motion of the B -meson in the CM. This requirement is not applied to off-resonance data.

The background due to initial state radiation with a hard photon (“radiative return to J/ψ ($\psi(2S)$)”) [6] and higher order QED processes $e^+e^- \rightarrow J/\psi \gamma^*$, $J/\psi l^+l^-$ [7] is also large. This background contributes mainly to $N_{\text{ch}} = 3$ and $N_{\text{ch}} = 4$ events, and a dedicated study was performed for each of these samples. The J/ψ mass peak for $N_{\text{ch}} = 3$ has a signal to background ratio $S/B \approx 0.1$, which is too poor to be included in the final signal sample. For $N_{\text{ch}} = 4$ the S/B ratio is acceptable, but 85% of the J/ψ mesons are due to QED processes, principally $e^+e^- \rightarrow \psi(2S) \gamma \rightarrow J/\psi \pi^+\pi^-$ (γ) with or without a visible photon. Based on this study we require $N_{\text{ch}} > 4$ to suppress the QED backgrounds, and account for the loss of low multiplicity signal events in the efficiency calculation. The remaining QED background in $N_{\text{ch}} > 4$ events is suppressed by rejecting events with a $\psi(2S) \rightarrow J/\psi \pi^+\pi^-$ candidate accompanied by either a photon with CM energy $E^* > 3.5$ GeV or electron tracks from photon conversion.

Mass distributions for prompt J/ψ candidates in the $\Upsilon(4S)$ and continuum data samples are shown in Fig. 1. Clear signals are observed both in the off-resonance (226 ± 23 events) and the $\Upsilon(4S)$ data (1459 ± 57 events), for both decay channels. The average detection efficiency for $J/\psi \rightarrow e^+e^-$ ($\mu^+\mu^-$) is 38% (48%).

The $\psi(2S)$ signal in $\Upsilon(4S)$ data with $p^* > 2$ GeV/ c is shown in Fig. 2(a). Combining $J/\psi \rightarrow e^+e^-$ and $\mu^+\mu^-$, a clear signal of 143 ± 19 events is seen in the mass difference $M_{l^+l^-\pi^+\pi^-} - M_{l^+l^-}$ distribution. In the off-resonance data, no statistically significant $\psi(2S)$ signal is seen (10 ± 5 events); this is not inconsistent with the observed rate at the $\Upsilon(4S)$ resonance. Searching for χ_{c1} and χ_{c2} in the $\Upsilon(4S)$ data, we form the mass difference $M_{l^+l^-\gamma} - M_{l^+l^-}$; no significant signals are seen (Fig. 2(b)). The average detection efficiency for $\psi(2S)$ and χ_{c1} , χ_{c2} is 20% and 21% respectively.

We first compare J/ψ production for $p^* > 2$ GeV/ c in the $\Upsilon(4S)$ and continuum data samples by extracting the number of signal events from invariant mass distributions for 300 MeV/ c wide p^* bins. The shape and normalization of the resulting p^* distribution for the off-resonance continuum (not shown) agree very well with those for the $\Upsilon(4S)$ data, indicating that all the J/ψ production at the $\Upsilon(4S)$ can be explained by continuum production. The branching fraction for the decay $\Upsilon(4S) \rightarrow J/\psi X$ can be estimated from the difference between the normalized yields (1459 ± 57 and 1496 ± 145 from the $\Upsilon(4S)$ and off-resonance data respectively) which is found to be -37 ± 156 . We therefore set an upper limit $\mathcal{B}(\Upsilon(4S) \rightarrow J/\psi X) < 1.9 \times 10^{-4}$ (at 95% C.L.) using the Feldman-Cousins method [9]. This limit is more stringent than the result of Ref. [10]. There are no published predictions for $\mathcal{B}(\Upsilon(4S) \rightarrow J/\psi X)$, but scaling the NRQCD estimate $\mathcal{B}(\Upsilon(1S) \rightarrow J/\psi X) \sim 4.5 \times 10^{-4}$ [11] by the ratio of widths $\Gamma_{\Upsilon(1S)}/\Gamma_{\Upsilon(4S)}$ gives $\sim 1.7 \times 10^{-6}$; this is far below our current experimental sensitivity.

Hereafter we assume that all prompt J/ψ 's produced at $\sqrt{s} \approx 10.6$ GeV are due to continuum production. We combine off-resonance data with the $\Upsilon(4S)$ data for $p^* > 2$ GeV/ c to extract charmonium production cross-sections and angular distributions. Acceptance corrections are determined using a dedicated Monte Carlo (MC) simulation of the process $e^+e^- \rightarrow J/\psi(\psi(2S))q\bar{q}$, where the composition of $q\bar{q}$ flavors is set to that observed at $\sqrt{s} \approx 10.6$ GeV. To minimize model dependence of the efficiency determination, the data is

corrected using a two-dimensional acceptance weight matrix as a function of p^* and $\cos\theta^*$, where θ^* is the J/ψ production angle in the CM system. The momentum range $p^* > 2$ GeV/ c is divided into three bins, and $\cos\theta^*$ into five bins; the number of signal events in each two-dimensional bin is obtained by fitting the invariant mass distribution. A similar procedure is applied to determine the $\psi(2S)$ acceptance for $p^* > 2$ GeV/ c , while acceptance corrections for $\chi_{c1,c2}$ were estimated directly from the MC without binning.

The resulting cross-sections are summarized in Table I. For the J/ψ sample ($p^* > 2$ GeV/ c), the feed-down from prompt $\psi(2S)$ is measured to be $0.33 \pm 0.04_{-0.06}^{+0.05}$ pb, and this contribution is subtracted to give the direct J/ψ cross-section in the table. The $p^* < 2$ GeV/ c off-resonance data is used to extend the J/ψ cross-section measurement to the full p^* range. As we observe no significant signal in the continuum for $\psi(2S)$, χ_{c1} and χ_{c2} , we estimate cross-sections for $p^* > 2$ GeV/ c only.

For the systematic errors of the measured cross-sections the following contributions are considered (where appropriate): uncertainty in the efficiency determination ($\pm 5\%$), effects of the multiplicity cut ($+4\%$), lepton identification ($\pm 4\%$), tracking ($\pm 4\%$), luminosity measurement ($\pm 1.3\%$), possible feed-down from the $\chi_{c1,c2}$ (-10%), contamination from QED processes (-4%), $\psi(2S)$ feed-down subtraction ($\pm 2\%$) and errors of the respective branching fractions. A contribution from the unobserved process $\Upsilon(4S) \rightarrow J/\psi X$ is not included. If the true branching fraction for this decay were just below the determined upper limit, the measured J/ψ cross-sections would be overestimated by ~ 0.18 pb. Other sources of systematic error, such as contamination from radiative return to the $\Upsilon(1S, 2S, 3S)$ and from $\gamma\gamma \rightarrow \chi_{c2}$, were found to be negligible. As an additional check, J/ψ cross-sections were determined separately for the e^+e^- and $\mu^+\mu^-$ decays, and found to be in good agreement: their ratio is $1.00 \pm 0.07 \pm 0.04$.

Our results on the J/ψ total and partial cross-section are smaller than those of BABAR [10]. The partial cross-sections for direct J/ψ and prompt $\psi(2S)$ production represent the first measurements in e^+e^- collisions.

NRQCD predictions for $\sigma(e^+e^- \rightarrow J/\psi_{\text{direct}} X)$ cover the range 0.8 – 1.7 pb [12] [13] [11]. (We exclude the extreme value of Ref. [7].) The most recent analysis [11] obtains a total cross-section of 0.8 – 1.1 pb, attributing 0.3 pb and 0.5 – 0.8 pb to color-singlet and color-octet mechanisms respectively. Our result can be used to further constrain the combination of color-octet matrix elements needed in the calculation [12] [11]. The ratio $\sigma(\psi(2S) X)/\sigma(J/\psi_{\text{direct}} X)$ is measured to be $0.93 \pm 0.11_{-0.15}^{+0.13}$; this is related in NRQCD to a ratio of linear combinations of non-perturbative matrix elements for the respective mesons [14].

Momentum distributions are shown in Fig. 3. The distribution of feed-down from $\psi(2S)$ to J/ψ is also shown in Fig. 3(a): it does not significantly modify the overall shape of the J/ψ momentum distribution. The J/ψ distribution vanishes ~ 300 MeV/ c below the kinematical limit (4.84 GeV/ c) while the $\psi(2S)$ momentum distribution extends till the end-point (4.65 GeV/ c). The J/ψ distribution is softer than the NRQCD prediction for color-singlet $J/\psi gg$ [15] [13], and agrees qualitatively with the predicted shape of the color-singlet $J/\psi c\bar{c}$ component [15] [13]. Some NRQCD calculations also predict a dramatic rise in the cross-section at the end-point due to color-octet $e^+e^- \rightarrow J/\psi g$ [16] [15]. The detection efficiency for this process was studied using a dedicated generator embedded in PYTHIA [17]. Assuming a 1 pb cross-section for this process, we expect > 300 events in the last two bins

of Fig. 3(a). No such signal is observed.

The distributions of the prompt J/ψ CM production angle θ^* , and the helicity angle θ_H (the angle between the positive lepton daughter momentum vector in the J/ψ rest frame, and the J/ψ momentum vector in the CM system), have also been studied in different momentum intervals. We correct the distributions for detection efficiency, but ignore possible effects due to feed-down. The distributions are fitted with the parameterizations $1 + A \cos^2 \theta^*$ and $1 + \alpha \cos^2 \theta_H$; the results are summarized in Table II, with selected fits also shown in Fig. 4. No statistically significant p^* dependence is seen for either A nor α parameters.

A large positive A at all momenta for direct J/ψ production is expected only for the color-singlet $J/\psi c\bar{c}$ mechanism [15]. However its contribution to the cross-section is thought to be small ($\sim 10\%$) [15] [13]. The leading color octet process $J/\psi g$ is expected to yield $A \approx +1$ at the endpoint [16] [15], although as noted above we do not observe these events in the p^* distribution. A significant longitudinal polarization of direct J/ψ mesons ($\alpha < -0.4$) is expected for the color-singlet process $J/\psi gg$ alone [13].

In summary, we have observed production of prompt J/ψ and $\psi(2S)$ at energies near the $\Upsilon(4S)$ mass. We set an upper limit for J/ψ production from $\Upsilon(4S)$ (valid for $p^* > 2 \text{ GeV}/c$), $\mathcal{B}(\Upsilon(4S) \rightarrow J/\psi X) < 1.9 \times 10^{-4}$ at the 95% C.L., and find the total cross-section for continuum prompt J/ψ production to be $\sigma(e^+e^- \rightarrow J/\psi X) = 1.47 \pm 0.10(\text{stat.}) \pm 0.13(\text{syst.}) \text{ pb}$. In the momentum range $p^* > 2 \text{ GeV}/c$, we measure $\sigma(e^+e^- \rightarrow J/\psi_{\text{direct}} X) = 0.72 \pm 0.08_{-0.17}^{+0.13} \text{ pb}$ and $\sigma(e^+e^- \rightarrow \psi(2S) X) = 0.67 \pm 0.09_{-0.11}^{+0.09} \text{ pb}$, and their ratio $\sigma(\psi(2S) X)/\sigma(J/\psi_{\text{direct}} X) = 0.93 \pm 0.17_{-0.15}^{+0.13}$. The angular distribution of prompt J/ψ mesons follows $1 + A \cos^2 \theta^*$ with $A = 0.9 \pm 0.2$, and the helicity angle follows $1 + \alpha \cos^2 \theta_H$ with $\alpha = -0.4 \pm 0.1$ indicating partial longitudinal polarization. We do not observe a statistically significant variation of A or α with momentum.

We wish to thank the KEKB accelerator group for the excellent operation of the KEKB accelerator. We acknowledge support from the Ministry of Education, Culture, Sports, Science, and Technology of Japan and the Japan Society for the Promotion of Science; the Australian Research Council and the Australian Department of Industry, Science and Resources; the Department of Science and Technology of India; the BK21 program of the Ministry of Education of Korea and the CHEP SRC program of the Korea Science and Engineering Foundation; the Polish State Committee for Scientific Research under contract No.2P03B 17017; the Ministry of Science and Technology of Russian Federation; the National Science Council and the Ministry of Education of Taiwan; and the U.S. Department of Energy.

REFERENCES

- [1] G.T. Bodwin, E. Braaten and G.P. Lepage, Phys. Rev. D **51**, 1125 (1995).
- [2] For a recent review see, M. Kramer, hep-ph/0106120, Prog. Part. Nucl. Phys. (to be published).
- [3] This Letter updates results first presented by T. Kawasaki, in proceedings of the BCP4 Conf., Ise-Shima, 2001 (to be published); see also K. Abe *et al.*, BELLE-CONF-0128, contributed to the EPS HEP 2001 and Lepton Photon '01 conferences.
- [4] KEKB B Factory Design Report, KEK Report 95-1, 1995, unpublished.
- [5] K. Abe *et al.* (Belle Collaboration), KEK Report 2000-4, to be published in Nucl. Inst. and Methods.
- [6] M. Benayoun, S.I. Eidelman, V.N. Ivanchenko, and Z.K. Silagadze, Mod. Phys. Lett. A **14**, 2605 (1999).
- [7] C.-H. Chang, C.-F. Qiao, and J.-X. Wang, Phys. Rev. D **57**, 4035 (1998).
- [8] T. Skwarnicki, Ph.D. Thesis, Institute of Nuclear Physics, Krakow 1986; DESY Internal Report, DESY F31-86-02 (1986).
- [9] G.J. Feldman and R.D. Cousins, Phys. Rev. D **57**, 3873 (1998).
- [10] B. Aubert *et al.* (BABAR Collaboration), Phys. Rev. Lett. **87**, 162002 (2001).
- [11] G.A. Schuler, Eur. Phys. J. C **8**, 273 (1999).
- [12] F. Yuan, C.-F. Qiao and K.-T. Chao, Phys. Rev. D **56**, 321 (1997); **56**, 1663 (1997).
- [13] S. Baek, P. Ko, J. Lee, and H.S. Song, J. Kor. Phys. Soc. **33**, 97 (1998); hep-ph/9804455.
- [14] E. Braaten, B.A. Kniehl and J. Lee, Phys. Rev. D **62**, 094005 (2000).
- [15] P. Cho and A.K. Leibovich, Phys. Rev. D **54**, 6690 (1996).
- [16] E. Braaten and Yu-Qi Chen, Phys. Rev. Lett. **76**, 730 (1996).
- [17] T. Sjöstrand, PYTHIA 5.7 / JETSET 7.4, CERN-TH.7112/93 (1993); T. Sjöstrand, Comp. Phys. Commun. **82**, 74 (1994).

TABLES

TABLE I. The measured charmonium cross-sections. The upper limits for χ_{c1} and χ_{c2} are at the 90% C.L.

σ [pb]	$0 < p^* < p_{max}^*$ [GeV/c]	$2.0 < p^* < p_{max}^*$ [GeV/c]
$\sigma(e^+e^- \rightarrow J/\psi X)$	$1.47 \pm 0.10 \pm 0.13$	$1.05 \pm 0.04 \pm 0.09$
$\sigma(e^+e^- \rightarrow J/\psi_{\text{direct}} X)$	—	$0.72 \pm 0.08^{+0.13}_{-0.17}$
$\sigma(e^+e^- \rightarrow \psi(2S) X)$	—	$0.67 \pm 0.09^{+0.09}_{-0.11}$
$\sigma(e^+e^- \rightarrow \chi_{c1} X)$	—	< 0.35
$\sigma(e^+e^- \rightarrow \chi_{c2} X)$	—	< 0.66

TABLE II. Results of the fits to angular distributions.

$p_{J/\psi}^*$ [GeV/c]	A	$\chi^2/\text{d.o.f.}$	α	$\chi^2/\text{d.o.f.}$
2.0 – 2.6	$0.3^{+0.5}_{-0.4}$	1.5/4	-0.4 ± 0.2	7.8/4
2.6 – 3.4	$1.1^{+0.4}_{-0.3}$	5.0/4	-0.4 ± 0.1	1.3/4
3.4 – 4.9	$1.1^{+0.4}_{-0.3}$	4.5/4	-0.2 ± 0.2	7.1/4
2.0 – 3.4	0.7 ± 0.3	1.2/4	-0.5 ± 0.1	4.6/4
2.0 – 4.9	0.9 ± 0.2	3.0/4	-0.4 ± 0.1	13.4/4

FIGURES

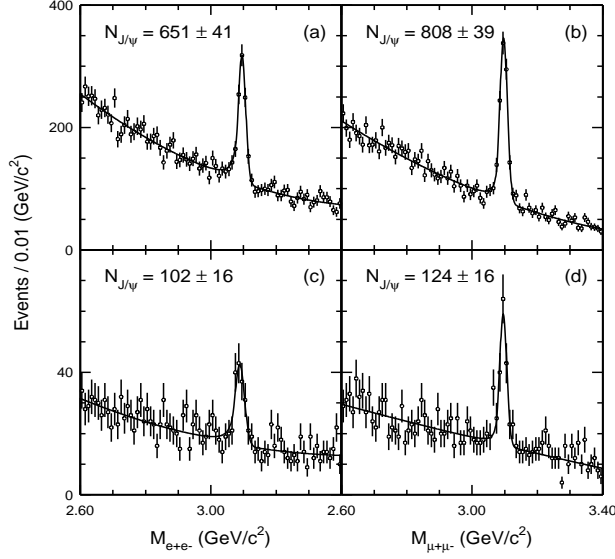


FIG. 1. Mass distributions for the $J/\psi \rightarrow e^+e^-$ (a,c) and $\mu^+\mu^-$ (b,d) candidates; (a) and (b) are for $\Upsilon(4S)$ data with $p^* > 2$ GeV/c, (c) and (d) are for off-resonance data. $N_{J/\psi}$ is the number of J/ψ mesons determined by a fit to the dilepton mass distribution, where a Crystall Ball line shape function [8] is used for the signal and the background is described by a polynomial.

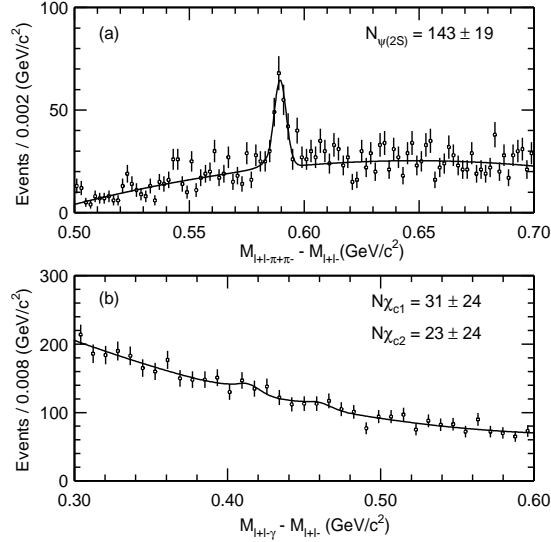


FIG. 2. Mass difference distributions for charmonium candidates in the $\Upsilon(4S)$ data: (a) $M_{l+l-\pi+\pi-} - M_{l+l-}$ for $\psi(2S)$ candidates with $p^* > 2$ GeV/c. (b) $M_{l+l-\gamma} - M_{l+l-}$ for $\chi_{c1,c2}$ candidates with $p^* > 2$ GeV/c. The curves represent fit results with a Crystall Ball line shape for the signal and a polynomial for the background.

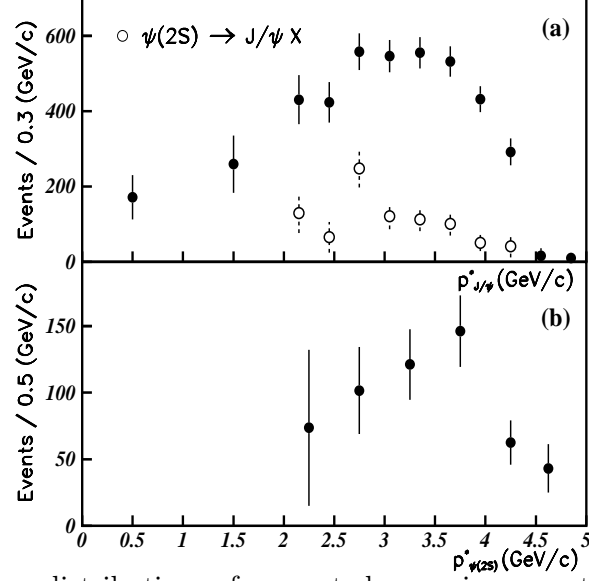


FIG. 3. CM momentum distributions of prompt charmonia, corrected for efficiency : (a) J/ψ (filled points) and J/ψ mesons from $\psi(2S) \rightarrow J/\psi X$ (open points); (b) $\psi(2S)$.

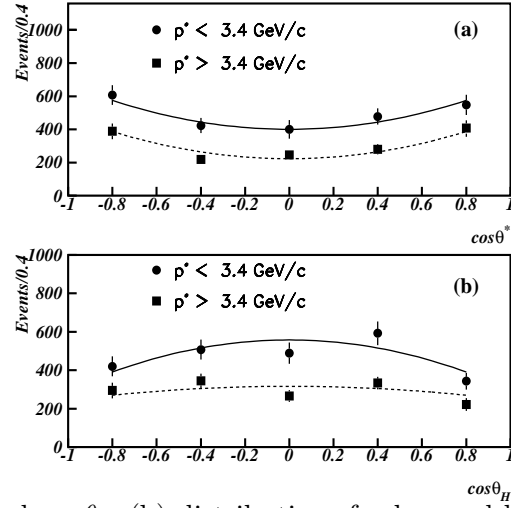


FIG. 4. The $\cos\theta^*$ (a) and $\cos\theta_H$ (b) distributions for low and high p^* . The curves represent fit results, described in the text and summarized in Table II.